Low-dose statin effects on α-dystroglycan O-mannosylation and other terpene biosynthesis-dependent pathways in mammalian muscle cells

By

Amr Mohamaden Abdelkader Mohamed

Thesis submitted to

Bonn-Rhein-Sieg University of Applied Sciences

Department of Natural Sciences

For the degree of

Master of Biomedical Sciences

https://doi.org/10.18418/opus-8274

1. Abstract

Statins are a group of hypolipidemic drugs that act by competitive inhibition of the HMGR enzyme. They are generally considered effective and safe but claimed to have side effects on skeletal muscles. A molecular side effect of statins is the block of terpene biosynthesis and hence of dolichol involved in N-glycosylation and O-mannosylation of proteins. Defects in O-mannosylation lead to α-dystroglycan (α-DG) hypoglycosylation and a series of hereditary dystroglycanopathies. The current project aims to get insight into molecular pathomechanisms induced by statins in mammalian muscle cells and to unravel a potential link between these effects and statin-induced decreases of α-DG O-mannosylation. The study was based on mass spectrometric proteomics supported by western blot analysis to reveal Rosuvastatin effects on cellular pathways under high (micromolar) or low (nanomolar) conditions. Differential proteomics revealed higher statin effects on muscle cell function in micromolar than nanomolar concentration, which is reached in the patient's plasma. We demonstrated distinct and partially overlapping patterns of fold-changed proteins under high and low statin conditions. Gene ontology term enrichment (GOTE) analyses of fold-changed proteins revealed cellular pathways related to muscle function and development are affected, even under low statin conditions, typically reached in the patient's plasma during prophylactic medication.

Table of Contents

1. Abstract

Statins are a group of hypolipidemic drugs that act by competitive inhibition of the HMGR enzyme. They are generally considered effective and safe but claimed to have side effects on skeletal muscles. A molecular side effect of statins is the block of terpene biosynthesis and hence of dolichol involved in N-glycosylation and O-mannosylation of proteins. Defects in O-mannosylation lead to α-dystroglycan (α-DG) hypoglycosylation and a series of hereditary dystroglycanopathies. The current project aims to get insight into molecular pathomechanisms induced by statins in mammalian muscle cells and to unravel a potential link between these effects and statin-induced decreases of α-DG O-mannosylation. The study was based on mass spectrometric proteomics supported by western blot analysis to reveal Rosuvastatin effects on cellular pathways under high (micromolar) or low (nanomolar) conditions. Differential proteomics revealed higher statin effects on muscle cell function in micromolar than nanomolar concentration, which is reached in the patient's plasma. We demonstrated distinct and partially overlapping patterns of fold-changed proteins under high and low statin conditions. Gene ontology term enrichment (GOTE) analyses of fold-changed proteins revealed cellular pathways related to muscle function and development are affected, even under low statin conditions, typically reached in the patient's plasma during prophylactic medication.

2. Introduction

2.1 Statin-associated myopathy

Statins are a group of hypocholesterolemic drugs that indirectly reduce low-density lipoprotein (LDL) cholesterol and related cardiovascular diseases (Arora *et al*, 2006); thus, they effectively treat coronary artery disease (CAD) and hypercholesteremia. Statins are either synthetic (Atorvastatin, Cerivastatin, Fluvastatin, Pitavastatin, Rosuvastatin) or derived from fermentation (Lovastatin, Pravastatin, Simvastatin) or naturally occurring (Mevastatin).

In general, statins are considered effective and safe, though they are claimed to have myotoxic side effects. The pathogenesis of statin-induced myopathy is believed to arise from interference of multiple levels of protein modifications, including prenylation of protein, synthesis of selenoprotein, mitochondrial dysfunction, and dolichol biosynthesis (Vaklavas *et al*, 2009). At the same time, statins are known to have myalgia as the most common side effect, which affects about 1 out of 10 individuals treated with statins (Ramkumar *et al*, 2016).

The American College of Cardiology, together with the American Heart Association and the National Heart, Lung, and Blood Institute (ACC/AHA/NHLBI), states that myopathy is a general term relating to any muscle disease, which can be inherited or acquired (Bairey-Merz *et al*, 2002). Thus, we can define statin-associated myopathies as the diseases of the muscles associated as a side effect when treating patients with statins.

Even though statin-induced myopathy depends on statin dose, many predisposing factors (such as gender, age, hepatic dysfunction, renal insufficiency, hypothyroidism, metabolic muscle diseases, diabetes, and concomitant medication)

play an essential role as well, mainly by changing the metabolic processes and statins bioavailability (Thompson, 2003).

We chose Rosuvastatin (calcium) as an example of statins which was the seventh approved statin and approved by the United States Food and Drug Administration (FDA) in August 2003 under the brand name Crestor from AstraZeneca company. Rosuvastatin has low lipophilicity and hence lower cytochrome P450 catabolism, and that is why it is characterized by liver selectivity and fewer potential drug-drug interactions. Also, it is more effective than other statins for raising levels of LDL-C and lowering levels of LDL-C (Quirk *et al*, 2003).

2.2 Statins effect on the terpene biosynthetic pathway

Isoprenoids or terpenoids are a group of various lipophilic compounds built-up from isoprene five-carbon units, and they exist ubiquitously in all living organisms. These molecules are considered the most diverse and most extensive natural compounds family. Additionally, they have a central role (both functional and structural) within various biological processes such as gene expression regulation, electron transport, cell membranes formation, proteins modification, signal transduction pathways, and biosynthesis of many molecules as cholesterol, vitamins, and sex hormones (Jeong *et al*, 2018).

The terpene biosynthesis pathway is also known as the mevalonate-isoprenoid-cholesterol biosynthesis pathway. In summary, this pathway starts with activated acetic acid-acetyl-Co-A- which is converted to the trimeric β-hydroxymethylglutaryl CoA (HMG-CoA). HMG-CoA via HMG-CoA reductase (HMGR) enzyme is converted to mevalonate. The pathway branches later on into the cholesterol and terpene pathways, but the HMG-CoA reductase reaction is considered the rate-limiting step for both. In peroxysomes, isopentenyl pyrophosphate (IPP) is formed by

decarboxylation of a C6 precursor, and the C5 compound IPP is then used for the formation of the C10 geranyl pyrophosphate (GPP) and C15 farnesyl pyrophosphate (FPP) compounds, which is the branching point between biosynthesis of long-chain nonsterol and sterol synthesis as shown in **Figure 1** (Holstein & Hohl, 2004).

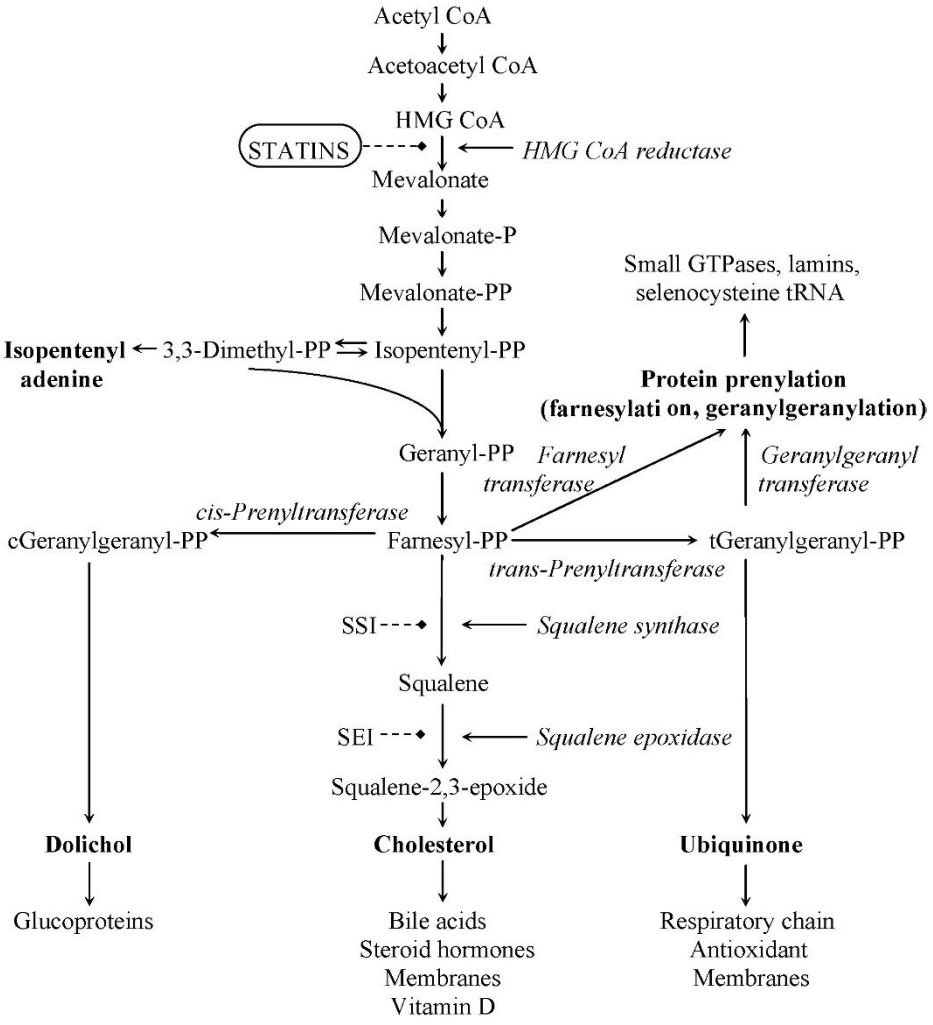

PP=Pyrophosphate, **SSI**=Squalene Synthase Inhibitors, **SEI**=Squalene Epoxidase Inhibitors

Figure 1. The mevalonate-isoprenoid-cholesterol biosynthesis pathway. *N.B. There is a typo in the word "Glycoproteins". Reprinted from Atherosclerosis, 202 /1, Christos Vaklavas, Yiannis S. Chatzizisis, Anthony Ziakas, Chrysanthos Zamboulis, George D. Giannoglou, Molecular basis of statin-associated myopathy, 18-28, Copyright (2009), with permission from Elsevier (License Number: 5166700712161).*

One compound formed from the precursor FPP is dolichol phosphate, a nonsterol isoprenoid lipid carrier involved in protein N-glycosylation and in the more rare O-mannosylation (Maciejak *et al*, 2013).

The statins do their effect by competitive inhibition of 3- hydroxy-3- methylglutaryl-coenzyme A (HMG-CoA) reductase, also known as β- hydroxy β-methylglutaryl-CoA reductase (HMGR). This enzyme located in the endoplasmic reticulum catalyzes the rate-limiting step of the terpene biosynthesis pathway, affecting most of the pathway products, both sterol and nonsterol isoprenoids (Istvan, 2001).

2.3 α-Dystroglycan O-mannosylation

α-Dystroglycan (α-DG) is a well-studied O-mannosylated protein which is cleaved from the dystroglycan precursor protein and forms the external subunit that is non-covalently linked to the membrane-associated subunit β-dystroglycan (β-DG). α-DG is post-translationally modified by peptide cleavage into the mature α-DG by furin (Sheikh *et al*, 2017).

α-DG is both N- and O-glycosylated; besides the classical mucin-type O-glycosylation (introduced later in the Golgi apparatus), the protein is also heavily modified in the endoplasmic reticulum (ER) by O-mannosylation of threonines or serines, which is crucial for its adequate function.

α-DG forms a bridge between extracellular matrix (ECM) proteins and the intracellular actin cytoskeleton via the dystrophin-glycoprotein complex (DGC), whereby the bridge formation is glycosylation dependent (Wells, 2013).

As statin has a molecular side effect due to the blockage of terpene biosynthesis, they also affect dolichol, which is involved in N-glycosylation and O-mannosylation of proteins. Dolichol is part of the α-dystroglycan (α-DG) mannosylation process; a blockage in the terpene biosynthesis pathway (specifically in dolichol formation) will

result in α-DG hypoglycosylation, which could be related to statins associated myopathy.

Defects in O-mannosylation lead to α-DG hypoglycosylation and compromise tissue structure, causing a series of dystroglycanopathies as in congenital muscular dystrophies (CMDs) (Praissman & Wells, 2014). Additionally, alpha-dystroglycan O-mannosylation plays a part in other diseases such as Arenaviridae family viral infection and metastasis of cancer (Dobson *et al*, 2013).

2.4 Functional enrichment and gene ontology enrichment analysis

Identifying the over-presentation of the association between specific terms and a list of genes (or gene products) is one of the robust methods in the bioinformatic evaluation of omics data. This enrichment analysis is a helpful tool to elaborate the massive data of proteomics experiments (Cantó - Pastor *et al*, 2021).

The Gene Ontology Consortium (GOC) provides a Gene Ontology (GO) enrichment analysis tool characterised by the broadest range of enrichment knowledge regarding genes and gene products. This tool is one of the gene enrichment tools for finding functionally related groups of genes or proteins obtained from a proteomics experiment, by using gene ontology terms to define biological processes, cellular components, or molecular functions (Carbon *et al*, 2021).

GO-Biological process enrichment analysis allows detecting genes or proteins contributing to biological processes or pathways to identify involved/affected pathways. This process is done by selecting and grouping functionally associated entities (proteins) in a structuring process where a single biological process could be fulfilled by one or more groups of molecular functions (Ashburner *et al*, 2000).

2.5 Aims

This work aims to identify pathways in mammalian muscle cells affected by blockage of terpene/ cholesterol synthesis using the HMG-CoA-reductase inhibitor Rosuvastatin.

Based on differential proteomics and supported by differential western blot analysis, the project aims to elucidate molecular pathomechanisms related to prolonged low-dose (nanomolar) and high-dose (micromolar) statin treatment and potentially associated with decreased O-mannosylation of α-dystroglycan.

The two concentrations, which were chosen in the current experimental series, are based on work from other laboratories (Maciejak *et al*, 2013; Göbel *et al*, 2015). Most reports on *in vitro* cell culture work refer to higher micromolar concentrations of statins (Xiao *et al*, 2018; Bonifacio *et al*, 2015; Sanvee *et al*, 2019; Schirris *et al*, 2015); however, it has been shown that the effective concentration in patients varies in the lower nanomolar range (Davidson, 2002). Accordingly, many effects reported in the literature, including those referring to effects on N-glycosylation of protein, could be based on statin concentrations, which are never reached in patients' blood.

Specifically, we wanted to address the potential link between O-mannosylation of α-DG and defects in muscle function or development since such a link is established for a series of hereditary dystroglycanopathies.

The scientific background of the project refers to the known side effects of statins on skeletal muscle by induction of muscle pain (myalgia), cramping, soreness, fatigue, weakness, and, in rare cases, rapid muscle breakdown that can lead to death.

3. Materials and methods

3.1 Materials

All information, including the manufacturers of materials used in this thesis work, is provided in tables 1 to 7.

3.1.1 Cell line

Prof. Dr. Marcus Krüger - CECAD provided the C2C12 immortalized mouse myoblast cell line.

3.1.2 Media for cell culture

Table 1. List of cell culture media used in this work.

Medium	Composition	Manufacturer
Growth medium	DMEM (1X) + GlutaMAX™-I (high glucose, no pyruvate)	Gibco - Thermo Fisher Scientific – (U.K.)
	1% L-Glutamine-Penicillin-Streptomycin solution	Sigma-Aldrich (Germany)
	10% FBS	Sigma-Aldrich (Germany)
Differentiation medium	DMEM (1X) + GlutaMAX™-I (high glucose, no pyruvate)	Gibco - Thermo Fisher Scientific – (U.K.)
	1% L-Glutamine-Penicillin-Streptomycin solution	Sigma-Aldrich (Germany)
	2% adult horse serum	Prof. Dr. Marcus Krüger group
Freezing medium	10% v/v DMSO In FBS	Sigma

3.1.3 Buffers

Table 2. List of buffers used in this work.

Name	Composition
1X PBS pH 7.4	140 mM NaCl

	10 mM Na_2HPO_4 2.7 mM KCl 1.2 mM KH_2PO_4
Lysis buffer	4% v/v SDS in PBS 50X protease inhibitor
1X SDS-PAGE running buffer	0.1% w/v SDS 25 mM Tris 250 mM glycine
1X TBS	150 mM NaCl 50 mM Tris-HCl pH 7.4
1X TBST	1X TBS 0.05% v/v Polysorbate 20 (Tween 20)
1X Transfer buffer	10% v/v Methanol 25 mM Tris 190 mM glycine
Urea buffer	8 M Urea in 50 mM TEAB
NuPAGE™ LDS Sample Buffer (4X) pH 8.5 (Invitrogen)	2% w/v LDS 10% v/v Glycerol 106 mM Tris HCl 141 mM Tris Base 0.22 mM SERVA Blue 0.51 mM EDTA 0.175 mM Phenol Red
Blocking buffer	5% w/v milk powder in TBST buffer

3.1.4 Chemicals

Table 3. List of chemicals used in this work.

Name	**Manufacturer**
Rosuvastatin calcium (≥ 98% - HPLC)	Sigma-Aldrich
Acetone, HPLC grade	Merck
TEAB	Sigma
DTT	Applichem
CAA	Merck

Formic acid	Honeywell/FLUKA
Buffer A: 0,1% v/v FA in water	VWR
Buffer B: 80% v/v ACN 0,1% v/v FA	Fisher scientific
Methanol LC-MS grade	VWR
Acrylamide-bis 30% (for electrophoresis)	Millipore -Merk-
SuperSignal™ West Dura Extended Duration Substrate	Thermo Fisher Scientific

3.1.5 Enzymes and antibodies

Table 4. List of enzymes and antibodies used in this work.

Name	Manufacturer
Trypsin, sequencing grade	Serva
Lysyl Endopeptidase (LysC)	WAKO
50x Protease Inhibitor cocktail	Roche
IIH6 primary antibody	Provided by Dr. med. Dipl. Chem. Sebahattin Cirak group
Goat anti-Mouse IgM Antibody, μ chain, horseradish peroxidase (HRP) conjugated secondary antibody	Merck Chemicals GmbH

3.1.6 Devices

Table 5. List of devices used in this work.

Name	Manufacturer
Q-Exactive Plus orbitrap coupled to EASY nLC 1000 UHPLC	Thermo Fisher Scientific (Germany)
Acclaim PepMap Rapid Separation Liquid Chromatography (RSLC) C18 column	Thermo Fisher Scientific (Germany)
BioPhotometer Model #6131	Eppendorf (Germany)
Vibracell 75115 Sonic Sonicator	Bioblock Scientific

LS6000 Cryogenic Sample Storage	Taylor-Wharton lab systems
ChemiDoc MP Imaging System	Bio-Rad (Germany)
CO2 incubator	Heraeus Deutschland
Sterile bank, safe 2020	Thermo Fisher Scientific (Germany)
Avanti series high-speed centrifuge	Beckman Coulter (Germany)
Heraeus Megafuge 13 centrifuge	Thermo Fisher Scientific (Germany)
Eppendorf 5415R Microcentrifuge	Eppendorf (Germany)
Thermomixer comfort	Eppendorf (Germany)
Mini-PROTEAN® Tetra Cell	Bio-Rad (Germany)
Mini Trans-Blot® Cell	Bio-Rad (Germany)
PowerPac™ Basic Power Supply	Bio-Rad (Germany)
Research plus pipettes	Eppendorf (Germany)

3.1.7 Consumables

Table 6. List of consumables used in this work.

Name	**Manufacturer**
SDB RP stageTip	CECAD Proteomics core facility, Cologne, Germany
Nitrocellulose membrane (0.45 µM)	GE-Healthcare
Cell culture T75 flasks	VWR

3.1.8 Software and online tools

Table 7. List of software and online tools used in this work.

Name	Application
MaxQuant (version 1.5.3.8) (Cox & Mann, 2008)	Analyzing large mass-spectrometric data sets
Perseus (version: 1.5.2.4) (Tyanova et al, 2016)	Evaluation of quantitative proteomics data, including various bioinformatic tools
Andromeda search engine (Cox et al, 2011)	MaxQuant Environment integrated Peptide Search Engine
GO Term Enrichment Analysis tool (provided by the Gene Ontology Consortium) released 2021-09-01: 43,850 (Ashburner *et al*, 2000; Carbon *et al*, 2021) powered by PANTHER Released 20210224 (Mi *et al*, 2013, 2021).	Gene Ontology enrichment analysis on genes or proteins sets
QuickGo: Explore biology web-based tool (Binns *et al*, 2009)	GO term slimming visualisation
Microsoft® Excel® for Microsoft 365 MSO (16.0.14228.20216) 64-bit	Analysis of M.S. data
Microsoft® PowerPoint® for Microsoft 365 MSO (16.0.14228.20216) 64-bit	Graphic representation of data

3.2 Methods

3.2.1 Cell culture of mouse muscle cells [1]

C2C12 cells were used (2 ml vials with 0.6 - 0.8 x 10^6 cells, passage 5). Vials were transferred to a T75 flask with a growth medium (see **Table 1**), incubated at 37°C - 5% CO_2, and passaged every two days without allowing cells to reach more than 70% confluence. Once the confluency reached 60%, cells were passaged to new T75 flasks with a split ratio between 1:5 to 1:10.

[1] Modified protocol from previous study (Günther *et al*, 2004).

The cells were passaged, washed with sterile PBS twice and incubated with trypsin for 10-15 minutes until a complete cell detachment was observed. Cells were resuspended thoroughly by pipetting up and down then examined under the microscope to avoid clumps.

Cells with trypsin solution were transferred from the T75 flask to a 15 ml falcon tube and centrifuged for 5 minutes at 1000 g. Cells had been counted using the Neubauer chamber, and the number of cells range was 1.4-1.8 x 10^6. Once the supernatant was discarded, the appropriate volume of fresh media was added depending on the splitting ratio to reach 10 ml total volume. Then cells were divided into 2ml vials by adding the freezing media and stored at -300° C (in nitrogen tank) for future use.

When passage nine was reached, the cells were cultured in two six-well plates, noting that only nine wells were used (three wells for each cell condition). The remaining three wells were negative control containing only medium to check for any contamination, as shown in **Figure 2**.

Cells were seeded by adding 2 ml of media containing cells to each well (2 ml of growth media in case of blank control) and placed into the incubator (37°C, 5% CO_2) until cell growth reached 90-100% confluency. The medium was switched to a differentiation medium (containing 2% horse serum compared to 10% FBS in growth medium) for three days, and the medium was replenished every 24 hours. Differentiation was confirmed under the microscope with a gradual increase in the fusion of the cells and formation of myotubes till the cell treatment started.

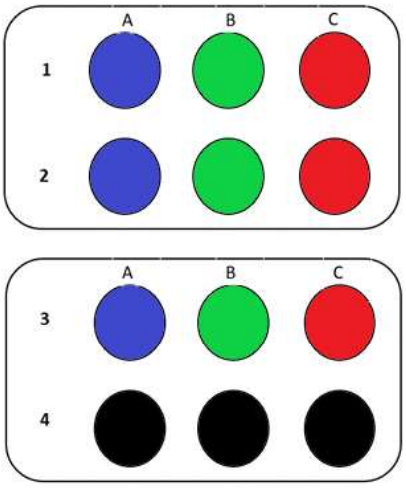

Figure 2. 6-Wells plate Cell culture. *Blue-coloured wells: non-treated cells (positive control). Green-coloured wells: 10 nM Rosuvastatin calcium treated cells (low concentration). Red-coloured wells: 10 µM Rosuvastatin calcium treated cells (high concentration). Black-coloured wells: blank media (negative control).*

3.2.2 Cell treatment with statin

Rosuvastatin was used to treat cells with high concentration (10 µM) and low concentration (10 nM). Rosuvastatin was added to the differentiation medium and was replenished every 24 hours for 72 hours.

3.2.3 Cell harvesting and lysis

After the third day, the medium was aspirated. Next, the cells were washed twice with cold PBS, then harvested using a cell scrubber in 1 ml cold PBS, transferred from the 6-wells plate to Eppendorf tubes 1.5 ml (one for each well), and centrifuged (1,000 x g., 5 minutes) before aspiration of the supernatant.

Cell lysis was performed in 1 ml lysis buffer for 5 minutes at 95°C. Chromatin was degraded using sonication (5 minutes, 15/15 seconds cycle, 25% amplitude).

The sample was cleared by centrifugation (15,000 x g., 10 minutes) before sample processing.

3.2.4 Protein acetone precipitation [2]

Ice cold acetone (4X volume) was added to the protein samples, followed by incubation at -80°C for 15 minutes and subsequently at -20°C for 120 minutes. Sample tubes were centrifuged at 16,000x g. for 15 minutes, and the supernatant was carefully removed. The step was repeated two times by adding 0.5 ml ice-cold acetone to the protein pellet, centrifuging at 16,000 x g. for 5 minutes. Lastly, the protein pellet was air-dried and resuspended in urea buffer.

3.2.5 Protein concentration estimation

Protein concentration was estimated by Ultraviolet (UV) absorption assay at 280 nm. 10 µl of the sample was diluted with PBS in a 1:20 ratio, and PBS solution was used as a control. Then, the protein concentration in the samples was estimated to be 1.4 - 1.8 mg ml^{-1}.

3.2.6 Proteins in-solution digestion [3]

50 µg from each sample were transferred to a new 1.5 ml Eppendorf tube. The reduction has been performed by adding dithiothreitol (DTT) to a final concentration of 5 mM. The sample was then vortexed and incubated for one hour at 25°C. Alkylation was performed using 40 mM chloroacetamide (CAA) and incubation for 30 minutes in the dark.

---

[2] Protocol obtained from (CECAD - Cluster of Excellence - University of Cologne), Acetone precipitation of proteins protocol, Version 4.0, http://proteomics.cecad-labs.uni-koeln.de/Protocols.955.0.html, December 15, 2017.

[3] Protocol obtained from (CECAD - Cluster of Excellence - University of Cologne), In solution digestion of proteins protocol, Version 3.2, http://proteomics.cecad-labs.uni-koeln.de/Protocols.955.0.html, August 1, 2018.

Lys-C was added with a 1:75 enzyme-to-substrate ratio, and the reaction mixture was incubated for four hours at 25°C. The sample was diluted with 50 mM TEAB to obtain a ≤ 2M final concentration of urea, followed by trypsin addition with a 1:75 enzyme-to-substrate ratio, and the sample was incubated overnight at 25°C.

The enzymatic digestion was terminated by acidifying the sample with formic acid to obtain a 1% v/v final concentration.

3.2.7 Desalting of peptides [4]

StageTips that contain two layers of styrenedivinylbenzol-reversed-phase sulfonate (SDB-RPS) were used for each sample.

In the first step, the stageTip was conditioned by adding 20 µl methanol to the stageTip then centrifuged for one minute at 600 x g. Next, the stageTip was equilibrated by adding 20 µl of 0.1% v/v formic acid in 80% v/v acetonitrile (buffer B) followed by centrifugation for one minute at 600 x g.

0.1% v/v Formic acid in water (buffer A) was added to the stageTip followed by centrifugation for 90 seconds. This step was repeated with increasing centrifugation time up to two minutes (till reach approximately 1-2 mm of buffer A on top of C18 material), and the collection tube was cleared from solvents.

In the sample purification step, the samples were centrifuged for five minutes at 16,100 x g.; then, the supernatant was loaded onto the stageTips, which were centrifuged for 5 minutes at 600 x g. The stageTips were washed with 30 µl buffer

[4] Protocol obtained from (CECAD - Cluster of Excellence - University of Cologne), SDB-RP StageTip purification of peptides protocol, Version 2.0, http://proteomics.cecad-labs.uni-koeln.de/Protocols.955.0.html, December 15, 2017.

A and centrifuged for three minutes at 600 x g.; the same step was repeated with buffer B twice. Lastly, the stageTips were completely dried using a syringe, stored at 4°C, and submitted to analysis by LC-ESI-MS in the CECAD Proteomics Facility.

3.2.8 Differential label-free LC-MS-based proteomics [5]

UHPLC-ESI-MS/MS analysis was performed on a Q-Exactive Plus Orbitrap connected with an EASY-nLC 1000 UHPLC. Samples were applied as 5 µl loads onto an Acclaim PepMap Rapid Separation Liquid Chromatography (RSLC) C18 column (150 mm length, 2 µm diameter beads, 100 A, internal diameter 50 µm). The flow rate was 200 nl $minute^{-1}$ in a gradient of buffer A (0.1% v/v formic acid in water) and buffer B (0.1% v/v formic acid in 80 % v/v acetonitrile), with increasing buffer B content from 2 % to 30% in 240 minutes and from 40 to 100% in 5 minutes.

The mass spectrometer was operated in a data-dependent mode with automatic switching between full-scan MS and MS/MS acquisition. The Orbitrap was adjusted to acquire Survey full-scan MS spectra (300−1800 m z^{-1}) with 70,000 resolution (200 m z^{-1}) after ions accumulation to a 3×10^6 target value depending on Automatic Gain Control (AGC) prediction from a previous full scan. The dynamic exclusion is set to 20 seconds. Twelve most intense multiply charged ions ($z \geq 2$) were consecutively isolated and fragmented by higher-energy collisional dissociation (HCD) together with a maximum injection time of 120 milliseconds in the octopole collision cell. The MS^2 (17,500 resolution) covered a - M+/-50 mass range and set the isolation width at 2.5 Daltons.

[5] This steps were done by CECAD Proteomics core Facility.

3.2.9 Data processing and evaluation

MaxQuant in the Perseus framework (MaxQuant version 1.5.3.8 - freely available software suite-) was used to process the raw M.S. files. The Andromeda search engine (Max-Quant framework included) was employed to search peak list files in databases with the following parameters: trypsin (full), minimum peptide length: 7, maximum missed cleavage sites: 2. Fixed modifications were cysteine carbamidomethylation; variable modifications were: peptide N-terminus acetylation and methionine oxidation. Target FDR values for peptides and proteins were set at 0.01 value.

Repeated-measures one-way ANOVA was conducted using Excel to statistically examine the effect of statin treatment under the three conditions (C, SM, SN).

Perseus (version: 1.5.2.4) was used to quantitatively evaluate the processed data and generate heatmap filtered for the ANOVA and Principal component analysis (PCA) graphs. PCA was performed in the Perseus framework as a largely parameter-free analysis according to the method mentioned in (Lever *et al*, 2017).

Three possible comparisons between the three groups (cell conditions) were t-tests calculated, which give the differences and significance for each comparison. Ratios were transformed to log2 values and normalized by subtracting the medians and recording the values within an Excel file. Proteins were classified as significantly changed in abundance if they exceeded a t-test difference > 1.0 or < -1.0 for increased abundance or decreased abundance, respectively.

The GOTE analysis tool (provided by the Gene Ontology Consortium and powered by Panther) was used to identify affected biological processes depending on the significantly fold-changed proteins.

Within the provided Excel file, the LC-MS results, there are two columns critical for further analysis: T-test difference between control (C) and high concentration treated cells (SM), t-test difference between control and low concentration treated cells (SN). These two columns were ordered subsequently in a descending way and significantly changed proteins were grouped with t-test difference > 1 for significantly increased abundance proteins and t-test difference < -1 for significantly decreased abundance proteins.

3.2.10 Gene Ontology Enrichment Analysis

The corresponding "Protein I.D.s" column in the excel file was then entered into the GOTE software tool using the parameters mentioned in **Table 8**. Pathways were identified as "biological processes" affected by the respective treatment (comparing SN vs C or SM vs C).

Table 8. GOTE analysis parameters.

Parameter	setting
Analysis Type	PANTHER Overrepresentation Test (Released 20210224)
Annotation Version and Release Date	GO Ontology database DOI: 10.5281/zenodo.5080993 Released 2021-07-02 (Carbon & Mungall, 2018)
Analyzed List	SM-C or SN-C
Reference List	Homo sapiens (all genes in the database)
Annotation Data Set	GO biological process complete
Test Type	FISHER
Correction	FDR
Results display	Only results for FDR P < 0.05

3.2.11 SDS-PAGE and Western blot [6]

Proteins samples were heated for ten minutes at 70°C with NuPAGE™ 1X lithium dodecyl sulfate (LDS) sample buffer containing 100 mM DTT and 7.5 µl of each sample (control, high concentration statin-treated and low concentration statin-treated). For SDS-PAGE analysis, they were subsequently loaded onto 6-15% v/v Tris-glycine gradient gel and separated at 95 volts for 30 minutes, followed by 120 volts.

After finishing the SDS-PAGE, the proteins were transferred from the polyacrylamide gels to GE-Healthcare nitrocellulose membranes (0.45 µM) in transfer buffer by applying 360 mA for 90 minutes at 4°C using an ice pack. Ponceau staining and image scanning were done to verify the transfer quality, and then the membrane was divided into two parts (for two primary antibody aliquots) and washed three times for 10 minutes each.

Next, the membrane surface was blocked for one hour at room temperature in the blocking buffer containing 5% w/v milk powder/TBST solution, then incubated with 1:250 α-dystroglycan IIH6 mouse anti-rabbit primary antibody in 5% w/v milk powder/TBST solution at 4°C overnight. The membrane was washed three times with TBST for 10 minutes each and transferred to a 1:1000 solution of goat-anti-mouse IgM horseradish peroxidase (HRP) conjugated secondary antibody (in 5% w/v milk powder/TBST) for 90 minutes at room temperature, then washed three times with TBST for 10 minutes.

[6] This step was done in cooperation with Dr. med. Dipl. Chem. Sebahattin Cirak group.

After washing three times with TBST, protein bands were detected by enhanced chemiluminescence (ECL) using SuperSignal™ West Dura Extended Duration Substrate by mixing the two solutions in equal volumes, placing them onto the membrane, and incubating for 5 minutes before analysis in a Bio-Rad Chemidoc Image system to detect the signals.

3.3 List of abbreviations:

Table 9. List of abbreviations.

Abbreviation	Explanation
LDL	Low-density lipoprotein
CAD	Coronary artery disease
ACC	American College of Cardiology
AHA	American Heart Association
NHLBI	National Heart, Lung, and Blood Institute
FDA	Food and Drug Administration
HMG-CoA	3- Hydroxy-3- methylglutaryl-Coenzyme A
HMGR	β- Hydroxy β-methylglutaryl-CoA reductase
IPP	Isopentenyl pyrophosphate
GPP	Geranyl pyrophosphate
FPP	Farnesyl pyrophosphate
α-DG	α-Dystroglycan
β-DG	β-Dystroglycan
ECM	Extracellular matrix
DGC	Dystrophin-glycoprotein complex
PBS	Phosphate-buffered saline
CECAD	Excellence Cluster for Cellular Stress Responses in Aging-Associated Diseases
DMEM	Dulbecco's Modified Eagle Medium
FBS	Fetal Bovine Serum
DMSO	Dimethyl sulfoxide
SDS	Sodium dodecyl sulfate
TBS	Tris-buffered saline
TEAB	Triethylammoniumbicarbonate
DTT	Dithiothreitol
CAA	Chloroacetamide
Lys-C	Lysyl Endopeptidase
nLC	Nano-liquid chromatography
UPLC	Ultra-Performance Liquid Chromatography
RSLC	Rapid Separation Liquid Chromatography
SDB	Styrenedivinylbenzol
RPS	Reversed-Phase Sulfonate
STAGETip	STop And Go Extraction Tip
GOTE	Gene Ontology Term Enrichment

AGC	Automatic Gain Control
HCD	Higher-energy collisional dissociation
FDR	False Discovery Rate
LDS	Lithium dodecyl sulfate
IgM	Immunoglobulin M
HRP	Horseradish peroxidase
ECL	Enhanced chemiluminescence
SM	10 µM Statin-treated C2C12 cells
SN	10 nM Statin-treated C2C12 cells
g.	G-force
v/v	Volume/volume
w/v	Weight/volume

4. Results

4.1 Differential label-free proteomics of C2C12 statin-treated and non-treated cells using LC-MS/MS

Mass spectrometry analysis of the three statin-treatment conditions identified 2340 proteins in C2C12 cells, of which 159 were significantly increased, and 644 were decreased in abundancies referring to micromolar concentration statin-treated cells (SM) versus control. On the other hand, 67 increased, and 263 proteins with decreased abundancies were identified in nanomolar concentration statin-treated cells (SN) versus control, as shown in **Figure 3**.

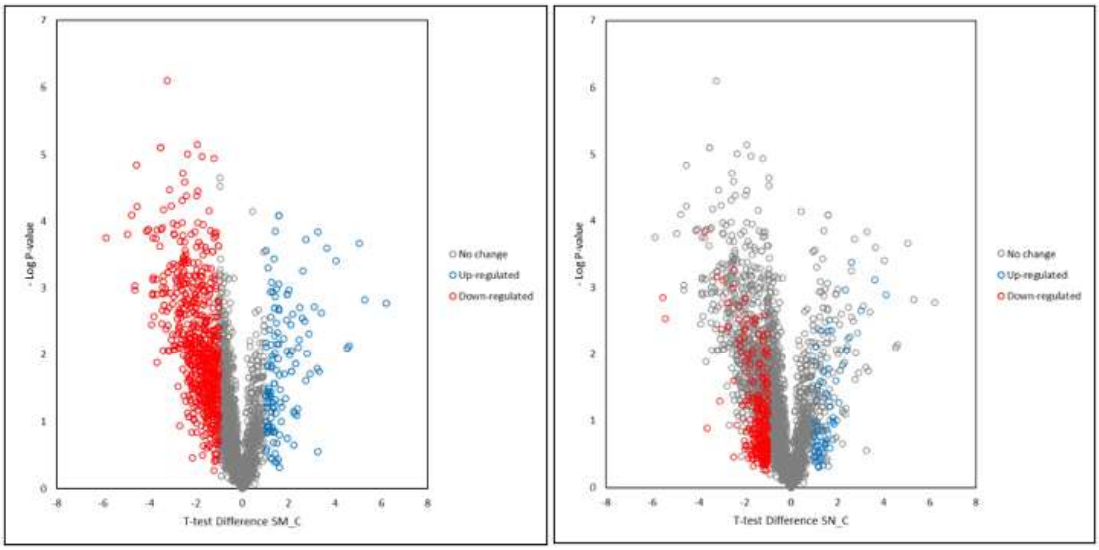

Figure 3. Volcano plot for MS analysis results. *SM: High concentration statin-treated cell samples, SN: Low concentration statin-treated samples, C: control samples.*

The one-way ANOVA (ANalysis Of Variance) with repeated measures was conducted on 2340 proteins to examine the effect on protein abundancies in muscle cells in the absence of statin and in the presence of low or high statin concentrations

(H_0: Cμ = SNμ = SMμ, H_1: Cμ ≠ SNμ ≠ SMμ). Results showed that the different statin concentrations lead to statistically significant differences in protein quantities where F- statistic (treatment conditions degree of freedom (df) = 2, error df = 4678) = 346.5985307, P-value < 4.3^{-141}.

For data variance examination, a heatmap filtered for ANOVA and principal component analysis (PCA) were conducted and indicated unexpected data clustering referring to SN-5 sample with the SM samples cluster rather than the SN samples cluster, thus representing an outlier as shown in **Figure 4**.

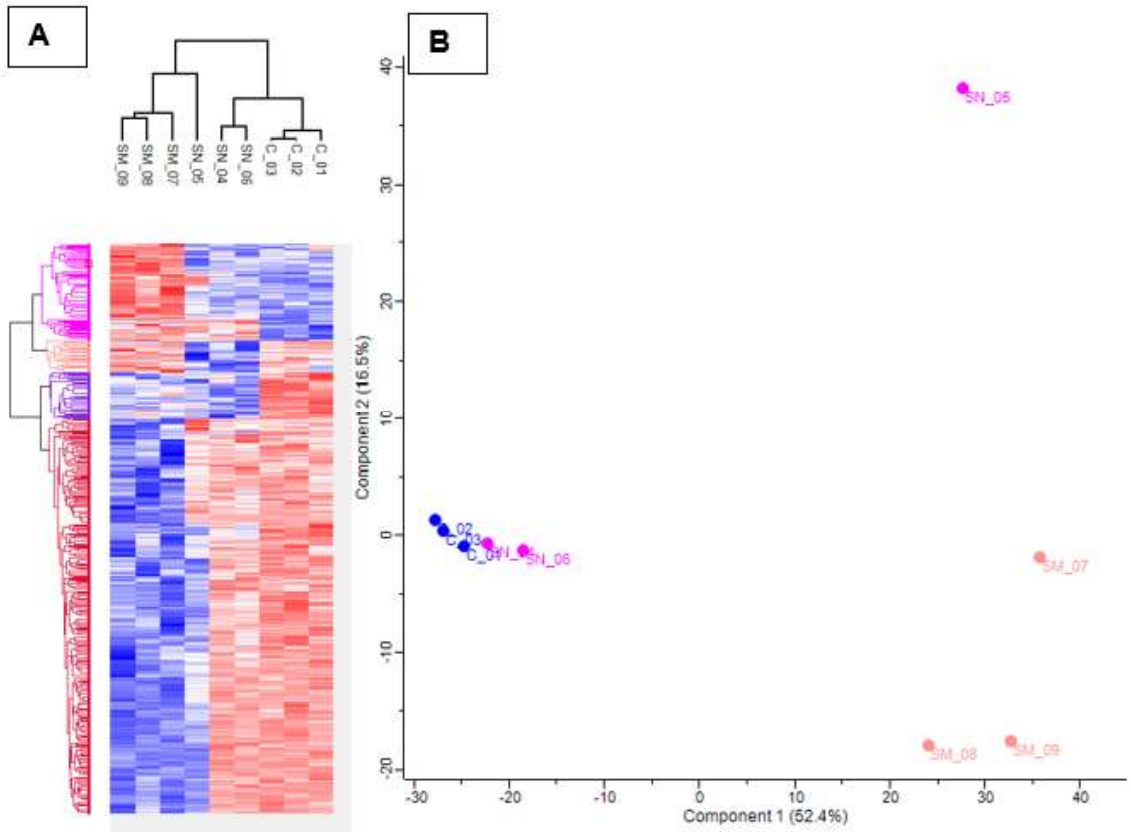

Figure 4. (A) Heatmap filtered for ANOVA. (B) PCA*. SM: High concentration statin-treated cell samples, SN: Low concentration statin-treated samples, C: control samples.*

To examine the difference between the high and low statin concentration treatment effect on protein glycosylation, significantly fold changed glycosylation-related proteins were filtered from others and shown in **Table 10**. The results indicate a significantly high abundance of two proteins Beta-sarcoglycan and Calreticulin, in the case of micromolar statin-treated condition only. However, another eight glycosylation-related proteins have a significantly lowered abundance only under a micromolar statin-treated condition. Only two proteins named N(4)-(beta-N-acetylglucosaminyl)-L-asparaginase, and Mannose-1-phosphate guanyltransferase beta have significantly low abundances in both micromolar and nanomolar statin treatment conditions.

Table 10. Glycosylation-related proteins with significant fold-changes. *nd: no significant difference. +: positive significantly fold change with t-test difference >1.0. -: Negative significantly fold change with t-test difference < -1.0.*

Protein ID	Protein names	N/C	M/C	Role
Q16585	Beta-sarcoglycan	nd	+	dystrophin-glycoprotein complex
P27797	Calreticulin	nd	+	protein-N-glycosylation control
P04844	Dolichyl-diphosphooligosaccharide-protein glycosyltransferase subunit 2	nd	-	N-glycosylation of proteins
P46977	Dolichyl-diphosphooligosaccharide-protein glycosyltransferase subunit STT3A	nd	-	N-glycosylation of proteins
Q8TCJ2	Dolichyl-diphosphooligosaccharide-protein glycosyltransferase subunit STT3B	nd	-	N-glycosylation of proteins
O15294	UDP-N-acetylglucosamine- peptide N-acetylglucosaminyltransferase 110 kDa subunit	nd	-	O-GlcNAcylation of proteins
Q10471	Polypeptide N-acetylgalactosaminyltransferase 2; Polypeptide N-	nd	-	O-glycosylation of proteins

	acetylgalactosaminyltransferase 2 soluble form			
Q9NYU2	UDP-glucose: glycoprotein glucosyltransferase 1	nd	-	O-Glucosylation of proteins
P07996	Thrombospondin-1	nd	-	O-glycosylation of proteins
O15305	Phosphomannomutase 2	nd	-	N- and O-glycosylation of proteins
P20933	N(4)-(beta-N-acetylglucosaminyl)-L-asparaginase; Glycosylasparaginase alpha chain; Glycosylasparaginase beta chain	-	-	GlcNAc-Asn glycosidase
Q9Y5P6	Mannose-1-phosphate guanyltransferase beta	-	-	N- and O-glycosylation of proteins

Moreover, to inspect the difference between micromolar and nanomolar statin conditions on the muscle function, significantly fold changed muscle function related proteins were examined and shown in **Table 11**.

Table 11. Muscle function-related proteins with significant fold-changes. *nd: no significant difference. +: positive significantly fold change with t-test difference >1.0. -: Negative significantly fold change with t-test difference < -1.0.*

Protein ID	Protein names	N/C	M/C
P60660	Myosin light polypeptide 6	nd	+
P19237	Troponin I, slow skeletal muscle	nd	-
P18206	Vinculin	nd	-
P35609	Alpha-actinin-2	nd	-
P45379	Troponin T, cardiac muscle	nd	-
O14983	Sarcoplasmic/endoplasmic reticulum calcium ATPase 1	nd	-
P48788	Troponin I, fast skeletal muscle	nd	-
Q6ZMU5	Tripartite motif-containing protein 72	nd	-
P13535	Myosin-8	nd	-
Q8WZ42	Titin	-	-
P20929	Nebulin	-	-
P13533	Myosin-6	-	-
P35749	Myosin-11	-	-

4.2 GOTE analysis for identifying affected biological processes

The GO term enrichment (GOTE) analysis for proteins with increased abundancies revealed a list of 60 and 25 biological processes in high statin- and low statin-treated cells, respectively, as shown in **Figure 5**.

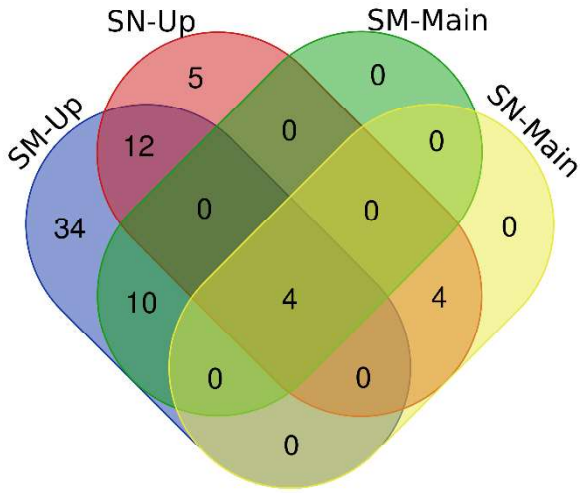

Figure 5. Venn chart presenting numbers of affected biological processes for increased abundancies proteins*. SM-Up: micromolar condition. SN-Up: nanomolar condition. SM-Main: parent biological process of micromolar condition. SN-Main: parent biological process of nanomolar condition.*

Within these listed processes, the 14 parent biological processes with the highest enrichment rates in the case of micromolar concentration statin-treated cells and 8 in nanomolar statin-treated cells are shown in **Figure 6**.

According to this analysis, the identified proteins with increased abundancies in both high and low-dose statin-treated cells compared to control are involved in negative regulation of chromatin silencing, nucleosome positioning, nucleosome assembly, and cytoplasmic translation biological processes. Other biological processes such as chromosome condensation, negative regulation of DNA recombination,

ribonucleoprotein complex assembly and mitochondrial transport appear only in the low statin concentration treated cells.

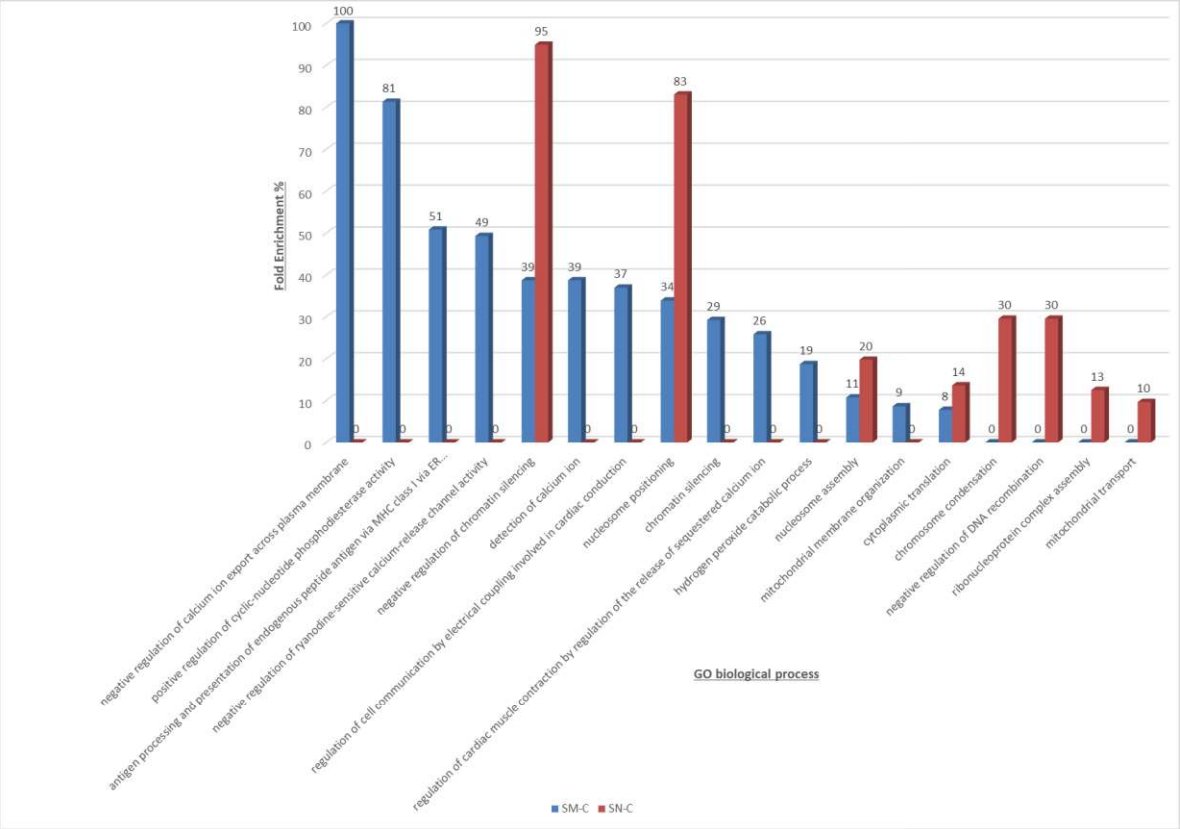

Figure 6. GOTE analysis results for up-regulated proteins. *SM-C: High concentration Vs. Control; SN-C: Low concentration Vs. control. N.B. "negative regulation of chromatin silencing" term appeared to be obsolete; which means it is removed from the published ontology as it is defined or named misleadingly, or describe a concept that is represented in other ways, or out of scope term* (The Gene Ontology Consortium).

Additionally, high statin-treated cells revealed many other unique biological processes are involved referring to proteins with increased abundancies, like negative regulation of calcium ion export across the plasma membrane, positive regulation of cyclic-nucleotide phosphodiesterase activity, antigen processing, and presentation of endogenous peptide antigen via MHC class I via ER pathway (TAP-

independent), negative regulation of ryanodine-sensitive calcium-release channel activity, detection of calcium ion, regulation of cell communication by electrical coupling involved in cardiac conduction, chromatin silencing, regulation of cardiac muscle contraction by regulation of the release of sequestered calcium ion, hydrogen peroxide catabolic process, and mitochondrial membrane organization.

On the other hand, GOTE analysis revealed more overlap in the listed biological processes affected in high or low-dose statin-treated cells, referring to proteins with decreased abundancies. 83 parent biological processes out of 371 were identified as affected in high-dose statin-treated cells. On the other hand, out of 143 biological processes, only 27 parent biological processes were indicated as affected in low-dose statin-treated cells, as shown in **Figure 7**.

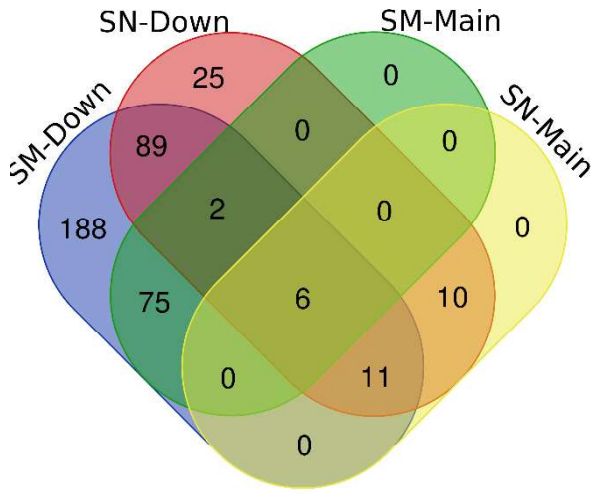

Figure 7. Venn chart presenting numbers of affected biological processes for decreased abundancies proteins. *SM-Up: micromolar condition. SN-Up: nanomolar condition. SM-Main: parent biological process of micromolar condition. SN-Main: parent biological process of micromolar condition.*

For ease of presentation, GOTE results for proteins with decreased abundance are shown as a list of the 30 most enriched biological processes with high enrichment

rates and related to muscle function, anatomy, or processes. The list contains 18 parent biological processes for high concentration statin-treated cells and 11 for low concentration statin-treated cells. The biological processes after the removal of 12 duplicates are shown in **Table 12** with the respective fold enrichment percentage.

Table 12. GOTE analysis results for proteins with decreased abundancies (30 most enriched processes for both SM and SN). *Muscle-related processes are marked in bold. SM-C: High concentration Vs. control. SN-C: Low concentration Vs. control. FE value: Fold Enrichment percentage value. #: parent process for SM. %: parent process for SN.*

GO biological process	FE value SM-C	FE value SN-C
Adenosine 5'-(hexahydrogen pentaphosphate) catabolic process #	25.82	0
Diadenosine hexaphosphate catabolic process #	25.82	0
Diadenosine pentaphosphate catabolic process #	25.82	0
Diphosphoinositol polyphosphate metabolic process #	25.82	0
Ddenosine 5'-(hexahydrogen pentaphosphate) metabolic process	25.82	0
Diadenosine hexaphosphate metabolic process	25.82	0
Diadenosine pentaphosphate metabolic process	25.82	0
Myosin filament assembly #	24	0
Regulation of twitch skeletal muscle contraction #	24	0
Myosin filament organization	24.21	0
Transition between fast and slow fiber #	23	0
Diadenosine polyphosphate catabolic process	21.52	0
Diadenosine polyphosphate metabolic process	21.52	0
Muscle filament sliding #	21	0
Positive regulation of microtubule nucleation #	20.18	0
Actin-myosin filament sliding	18.83	0
Positive regulation of miRNA mediated inhibition of translation #	18.45	0
Regulation of miRNA mediated inhibition of translation	18.45	0
UTP biosynthetic process #	16.14	0
GTP biosynthetic process #	14.67	0
Regulation of microtubule nucleation	14.67	0
UTP metabolic process	13.45	0
Pyrimidine ribonucleoside triphosphate biosynthetic process	12.91	0

Regulation of skeletal muscle adaptation	12.42	0
Pinocytosis #	11.74	0
Nuclear pore organization #	11.53	0
CTP biosynthetic process #	11.53	0
Negative regulation of protein localization to cell surface #	10.76	0
Regulation of pinocytosis #	10.76	0
Fibroblast migration #	11	0
Pyrimidine nucleoside triphosphate metabolic process %	9.04	12.67
Purine ribonucleoside monophosphate biosynthetic process %	8.49	16.68
Myofibril assembly %	7.79	8.19
GTP metabolic process %	7.75	12.67
Purine nucleoside monophosphate biosynthetic process	7.69	15.09
Striated muscle cell development	7.66	8.06
tRNA aminoacylation for protein translation %	6.92	9.43
tRNA aminoacylation	6.46	8.8
Amino acid activation	6.32	8.61
Ribonucleoside monophosphate biosynthetic process	5.7	11.65
Nucleoside monophosphate biosynthetic process	5.25	11.05
Cardiac muscle cell development %	4	8
Purine ribonucleoside monophosphate metabolic process	0	9.66
Negative regulation of calcium ion transmembrane transport %	0	9.66
Purine nucleoside monophosphate metabolic process	0	9
Purine ribonucleoside triphosphate biosynthetic process %	0	8.61
Oxidative phosphorylation	0	8.41
Ribonucleoside monophosphate metabolic process	0	8.06

Furthermore, to visualize the range of decreased abundances proteins, GOTE results were worked out through the QuickGo tool Explore Biology (a GO Slim search using GO terms I.D.s) (Binns *et al*, 2009).

Search results (proteins with decreased abundancies) obtained with the QuickGo slimming tool for the eight most enriched parent GO terms list differed between high and low-dose statin-treated cells. The QuickGo SM GO terms list resulted in 5 muscle-related parent biological processes, as shown in **Figure 8**. By contrast, the respective SN list comprised only two muscle-related parent biological processes, as shown in **Figure 9**.

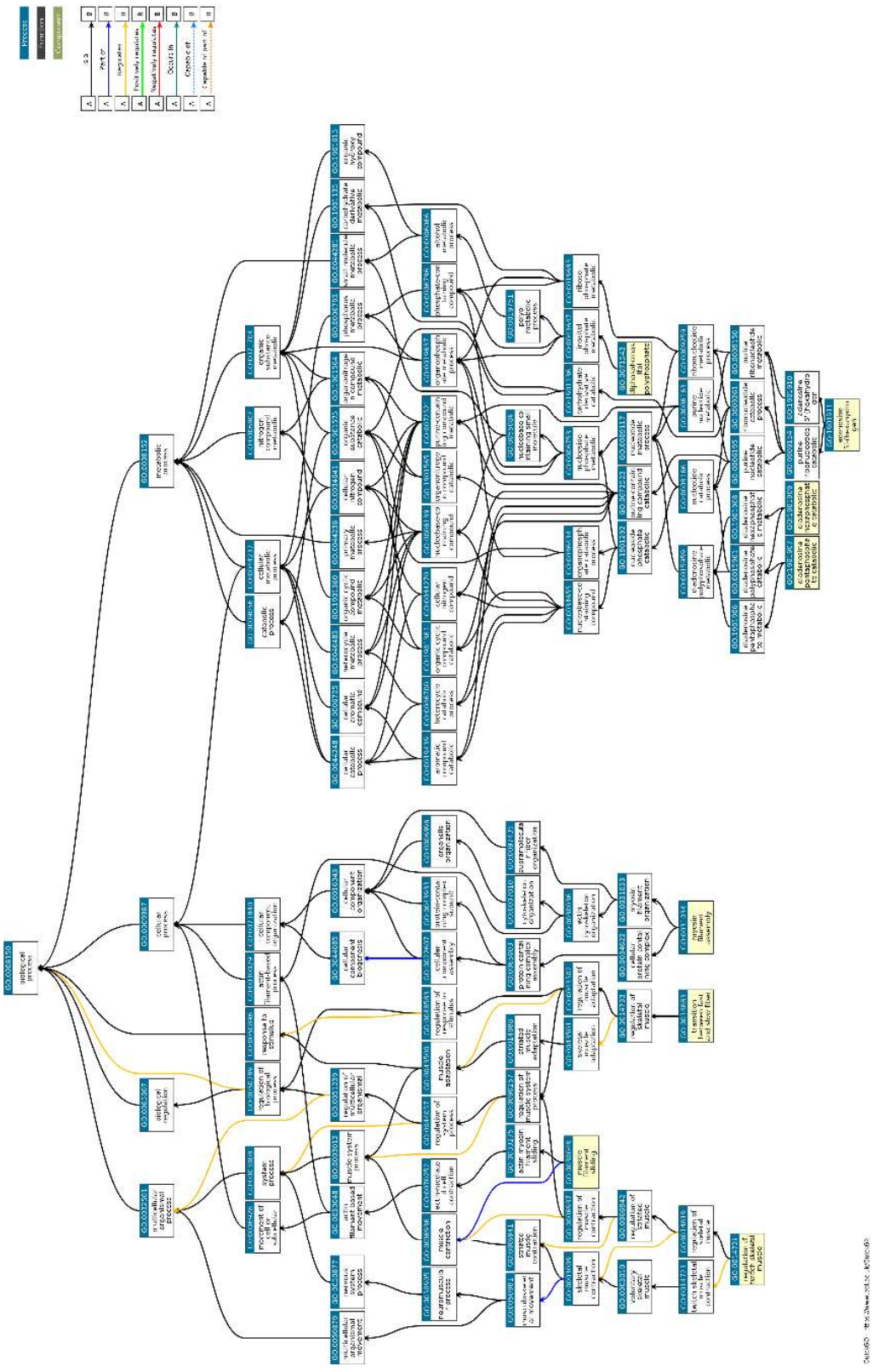

Figure 8. QuickGo slimming tool results for micromolar statin-treated cells with low abundant proteins. *Only the eight most enriched parent GO terms are shown in yellow-coloured boxes.*

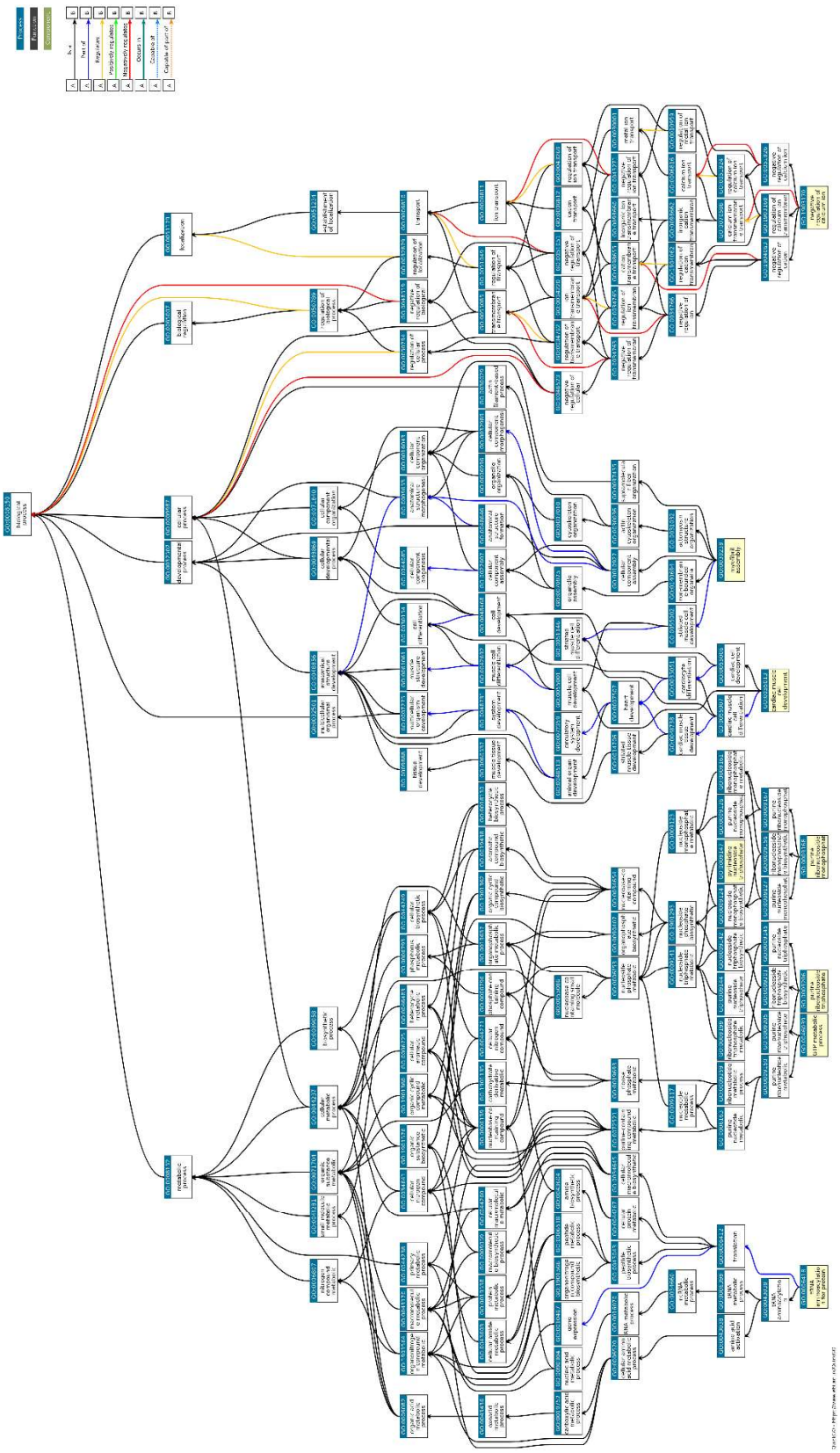

Figure 9. QuickGo slimming tool results for nanomolar statin-treated cells with low abundant proteins. *Only the eight most enriched parent GO terms are shown in yellow-coloured boxes.*

4.3 Westen blot

Western blots of samples under study were performed to get specific insight into a potential affection of α-DG O-mannosylation by statin treatment in different conditions.

Effectively O-mannosylated α-DG can be detected by IIH6 antibody, which requires a functional O-mannose epitope for the α-DG detection (Fortunato *et al*, 2014). This O-mannosylation specificity is the reason for our choice of IIH6 to demonstrate potential changes of O-mannosylation caused by statin-treatment with different concentrations.

On technically evaluating the blot quality, Ponceau S-stained patterns confirmed the efficient transfer of proteins from SDS-PAGE to the nitrocellulose membrane, as shown in **Figure 10**.

α-Dystroglycan is detected as a band at approximately 156 kDa, as shown in **Figure 11**. In all blots, the micromolar and nanomolar conditions showed increased O-mannosylation of α-DG compared to the control. There was almost no difference between the two statin-treatment conditions in technical replicate 2. However, the observed effect on O-mannosylation is not reproducible with aliquot number 1 of the same antibody.

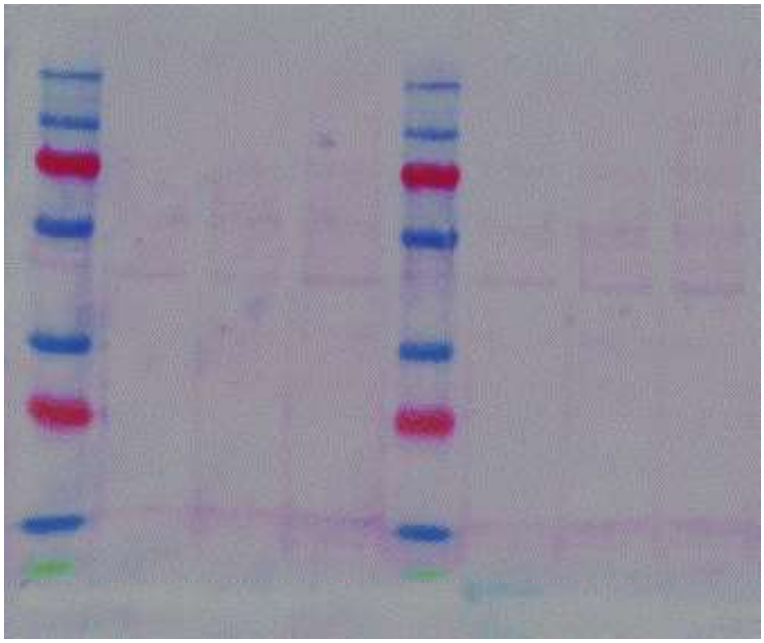

Figure 10. Ponceau S-stained blot.

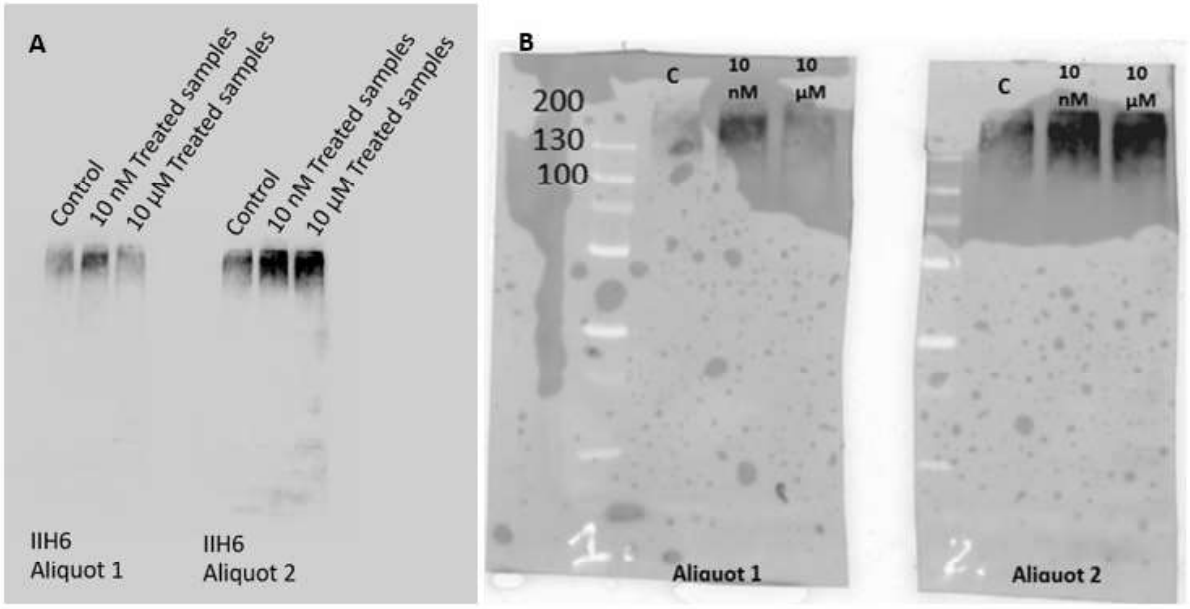

Figure 11. α-Dystroglycan O-mannosylation in high- and low-concentration statin-treated muscle cells. *(A) SDS-PAGE of control(C), 10nM (S.N.), and 10µM (S.M.) statin-treated samples western blot using two aliquots of IIH6 antibody and ECL for 5 seconds exposure. (B) SDS-PAG western blot Stain-free Image merged with 5 seconds exposure. C: control, S.N.: low concentration statin-treated cells, S.M.: high concentration statin-treated cells.*

5. Discussion

Results of this project emphasized that statin treatment at a micromolar concentration has a higher effect on the mammalian muscle cells than the nanomolar concentration reached in the patient's plasma. Also, statin treatment affected glycosylation-related and muscle function-related proteins more significantly during the high-dose statin treatment than low-dose statin treatment.

Even though many glycosylation-related proteins are significantly decreased in abundance when treated with Rosuvastatin, differential proteomics data did not reveal any direct relation between statin effects on muscle cell function and the terpene-dependent O-mannosylation of α-DG. Moreover, western blots of α-DG were not reproducible with different aliquots of the same antibody, making an unequivocal evaluation impossible.

However, on the basis of differential proteomics and the identification of fold-changed glycosylation-related proteins, the effect of statin treatment on dolichol biosynthesis and O-mannosylation of proteins can not be excluded.

Some of the statin's side effects could be related to an affection of the terpene biosynthetic pathway (Vaklavas *et al*, 2009), especially with respect to lipid carriers, like dolichol, which is functionally related to protein N-glycosylation and O-mannosylation.

5.1 Differential label-free proteomics results overview

By looking into the number of significantly fold-changed proteins in cells treated with different concentrations of statin, it is evident that the high statin concentration led to more proteins with increased abundancies (159 proteins for high concentration versus 67 proteins for low concentration). The same holds true for proteins with

decreased abundancies (644 proteins for high concentration versus 263 proteins for low concentration statin). From these results, it can be concluded that the effective concentration of statins appears to play an important role with respect to muscle cell side effects.

Furthermore, the one-way repeated measures ANOVA statistical analysis revealed significant differences between the muscle cell proteomes analysed under three different conditions. However, the heatmap and PCA in **Figure 4** showed one of the low concentration statin-treated samples (SN5) as an outlier sample that clustered with the high concentration samples (SM). As the entire experimental set-up was replicated starting from cell culture, multiple steps could contribute to the technical variance.

The glycosylation-related proteins in **Table 10** indicate that protein glycosylation is mostly negatively affected with respect to N- and O-glycosylation. However, there are no hints of a direct affection of α-DG O-mannosylation. In particular, three enzyme subunits of the protein N-glycosyltransferase are down-regulated, however only under high-statin conditions. On the other hand, a component of the dystrophin complex, beta-sarcoglycan, is increased significantly, potentially as a response to the affection of alpha-dystroglycan.

Additionally, the muscle function related proteins in **Table 11** show a difference between the effect of micromolar and nanomolar concentration.

Examining differences between the different statin-treatment conditions, it is clear that alpha-dystroglycan did not significantly change between cell conditions. However, other muscle cell function-related proteins and glycosylation-related proteins are affected to a greater extent in the micromolar statin-treatment condition

than the nanomolar condition. These results emphasize the more substantial effect of high statin concentration on muscle cells compared to lower concentrations on many proteins with decreased abundancies.

High-dose statin significantly decreased two sarcomere proteins Troponin T (slow skeletal muscle) and Nebulin, while low-dose statin-treatment significantly induced a decrease of Nebulin only. These two proteins fulfil functions in thin filament contractility and thin filament integrity, respectively. A decrease of these two proteins in the presence of high-dose statin could lead to sarcomere damage and instability with deterioration of muscle function as a side effect. The current findings are directly in line with previous findings of others (Williams *et al*, 2021). The group identified the above two proteins as significantly decreased in myofibrillar myopathy diseased Warmblood horses (in humans, myofibrillar myopathy causes skeletal muscle weakness and degeneration).

5.2 Affected biological processes revealed by GOTE

The powerful tool of gene ontology term enrichment analysis for the identification of affected biological processes also confirmed that high concentration statin treatment of muscle cells has much stronger effects on biological processes than lower concentration. Moreover, high-dose statin condition changes more biological processes than the cell treatment under low-dose statin condition, which are more adapted to the situation in patients exhibiting serum concentrations of statins in the lower nanomolar range (Davidson, 2002).

A brief look through the results of the GOTE visualization using the QuickGo tool revealed that proteins with significant decreases in abundancies should impact pathways related to tissue development, cell differentiation, multicellular organism

development, multicellular organismal movement, muscle structure development, actin filament-based movement, nervous system process, musculoskeletal movement, and muscle system process.

In the case of high-dose statin treatment of muscle cell, the affected muscle-related pathways included striated muscle contraction, muscle contraction, muscle system process, actin-myosin filament sliding, striated muscle adaptation, actin cytoskeleton organization, and myosin filament organization. On the other hand, low concentration statin treatment affected muscle-related pathways included cardiac muscle cell differentiation, striated muscle cell differentiation, and actomyosin structure organization.

As shown in **Table 12**, high-dose statin treatment generally had a potent effect on muscle-related pathways in the fold enrichment value and number of affected pathways. Out of 10 high-ranking GO terms, only one term had a higher fold enrichment in low concentration than high concentration treatment (cardiac muscle cell development), two nearly equal fold enrichment terms (myofibril assembly, striated muscle cell development). The remaining seven terms (myosin filament assembly, regulation of twitch skeletal muscle contraction, myosin filament organization, transition between fast and slow fiber, muscle filament sliding, actin-myosin filament sliding, regulation of skeletal muscle adaptation) had high fold enrichment in high-dose statin-treated cells. However, these seven terms were not listed for low concentration statin-treated cells.

Some GOTE results for the high-dose statin-condition in this study are in agreement with a previous study (Ning et al, 2020), where similar down-regulated gene ontology terms (striated muscle contraction GO:0006941, muscle contraction

GO:0006936, and muscle system process GO:0003012) have been shown for sepsis-induced myopathy bioinformatic analysis.

Our findings are also in line with a previous study of diabetic foot ulcer (DFU) patients (Qian et al, 2021). The study showed three main GO biological processes terms related to DFU patients and suggested a potential angiogenesis regulation and inflammatory response activation pathomechanism. Two of the reported GO terms (muscle filament sliding and sarcomere organization) show fold changes in the current study for low-abundancies proteins under high-dose statin conditions. This similarity between DFU and statin-associated myopathy suggests that muscle development and function impairment could be shared in both conditions.

A study of affected genes in rheumatoid arthritis (RA) revealed the relation of RA to some biological processes, including muscle filament sliding, muscle contraction, cardiac muscle contraction, cardiac muscle contraction, and sarcomere organization (Wu *et al*, 2021). These GO terms match our study results for low-abundancies proteins under high-dose statin conditions.

5.3 Alpha-dystroglycan O-mannosylation elucidation by western blot

In summary, based on non-reproducible preliminary data from western blots, it is impossible to make clear conclusions with regard to statin-induced effects on α-DG O-mannosylation.

The western blot showed increased O-mannosylation of the α-dystroglycan both in high- and low-dose statin-treated cells when comparing the western blot signal intensities with control (untreated) cells even though it is slightly higher in high-dose than low-dose of statin-treated cells.

However, these results are challenging to interpret since it is not clear whether the control is reliable. Comparing only the SN versus SM, it appears that there is actually a decrease in O-mannosylation of the target protein, but this effect was not reproducible with another aliquot of the same antibody. Ongoing western blot experiments are being conducted to elucidate reliable and reproducible results.

5.4 Conclusion and outlook

Rosuvastatin effects on mammalian muscle cell proteomes were demonstrated to be concentration-dependent. Conclusions drawn from previous *in vitro* studies on cellular statin effects should be carefully reviewed with respect to the artificially high concentrations of statins used, which are never reached in the patients' bloodstream.

As the above-reported differential proteomics approach did not reveal clear-cut evidence for the affection of alpha-dystroglycan O-mannosylation, complementary metabolomics and glycomics studies should give more conclusive insight into the possible affection of dolichol- and glycosylation-dependent pathways. To unravel, which signal transduction pathways are involved in the mediation of statin effects, a phosphopeptidomics experiment could be envisaged.

6. References

Arora R, Liebo M & Maldonado F (2006) Statin-induced myopathy: The two faces of janus. *J Cardiovasc Pharmacol Ther* 11: 105–112

Ashburner M, Ball CA, Blake JA, Botstein D, Butler H, Cherry JM, Davis AP, Dolinski K, Dwight SS, Eppig JT, *et al* (2000) Gene Ontology: tool for the unification of biology. *Nat Genet* 25: 25–29

Bairey-Merz CN, Grundy SM & Cleeman JI (2002) ACC / AHA / NHLBI CLINICAL ADVISORY ON STATINS ACC / AHA / NHLBI Clinical Advisory on the Use and Safety of Statins. *J Am Coll Cardiol* 40: 568–573 [PREPRINT]

Binns D, Dimmer E, Huntley R, Barrell D, O'Donovan C & Apweiler R (2009) QuickGO: a web-based tool for Gene Ontology searching. *Bioinformatics* 25: 3045–3046

Bonifacio A, Sanvee GM, Bouitbir J & Krähenbühl S (2015) The AKT/mTOR signaling pathway plays a key role in statin-induced myotoxicity. *Biochim Biophys Acta - Mol Cell Res* 1853: 1841–1849

Cantó - Pastor A, Mason GA, Brady SM & Provart NJ (2021) Arabidopsis bioinformatics: tools and strategies. *Plant J*

Carbon S, Douglass E, Good BM, Unni DR, Harris NL, Mungall CJ, Basu S, Chisholm RL, Dodson RJ, Hartline E, *et al* (2021) The Gene Ontology resource: enriching a GOld mine. *Nucleic Acids Res* 49: D325–D334

Carbon S & Mungall C (2018) Gene Ontology Data Archive.

CECAD - Cluster of Excellence - University of Cologne Proteomics Core facility website: Lab Protocols.

Cox J & Mann M (2008) MaxQuant enables high peptide identification rates, individualized p.p.b.-range mass accuracies and proteome-wide protein quantification. *Nat Biotechnol* 26: 1367–1372

Cox J, Neuhauser N, Michalski A, Scheltema RA, Olsen J V. & Mann M (2011) Andromeda: A Peptide Search Engine Integrated into the MaxQuant Environment. *J Proteome Res* 10: 1794–1805

Davidson MH (2002) Rosuvastatin: a highly efficacious statin for the treatment of dyslipidaemia. *Expert Opin Investig Drugs* 11: 125–141

Dobson CM, Hempel SJ, Stalnaker SH, Stuart R & Wells L (2013) O-Mannosylation and human disease. *Cell Mol Life Sci* 70: 2849–2857

Fortunato MJ, Ball CE, Hollinger K, Patel NB, Modi JN, Rajasekaran V, Nonneman DJ, Ross JW, Kennedy EJ, Selsby JT, *et al* (2014) Development of Rabbit Monoclonal Antibodies for Detection of Alpha-Dystroglycan in Normal and Dystrophic Tissue. *PLoS One* 9: e97567

Göbel A, Browne AJ, Thiele S, Rauner M, Hofbauer LC & Rachner TD (2015) Potentiated suppression of Dickkopf-1 in breast cancer by combined administration of the mevalonate pathway inhibitors zoledronic acid and statins. *Breast Cancer Res Treat* 154: 623–631

Günther S, Mielcarek M, Krüger M & Braun T (2004) VITO-1 is an essential cofactor of TEF1-dependent muscle-specific gene regulation. *Nucleic Acids Res* 32: 791–802

Holstein SA & Hohl RJ (2004) Isoprenoids: Remarkable diversity of form and function. *Lipids* 39: 293–309

Istvan ES (2001) Structural Mechanism for Statin Inhibition of HMG-CoA Reductase. *Science (80-)* 292: 1160–1164

Jeong A, Suazo KF, Wood WG, Distefano MD & Li L (2018) Isoprenoids and protein prenylation: implications in the pathogenesis and therapeutic intervention of Alzheimer's disease. *Crit Rev Biochem Mol Biol* 53: 279–310

Lever J, Krzywinski M & Altman N (2017) Principal component analysis. *Nat Methods* 14: 641–642

Maciejak A, Leszczynska A, Warchol I, Gora M, Kaminska J, Plochocka D, Wysocka-Kapcinska M, Tulacz D, Siedlecka J, Swiezewska E, *et al* (2013) The effects of statins on the mevalonic acid pathway in recombinant yeast strains expressing human HMG-CoA reductase. *BMC Biotechnol* 13: 68

Mi H, Ebert D, Muruganujan A, Mills C, Albou L-P, Mushayamaha T & Thomas PD (2021) PANTHER version 16: a revised family classification, tree-based classification tool, enhancer regions and extensive API. *Nucleic Acids Res* 49: D394–D403

Mi H, Muruganujan A, Casagrande JT & Thomas PD (2013) Large-scale gene function analysis with the PANTHER classification system. *Nat Protoc* 8: 1551–1566

Praissman JL & Wells L (2014) Mammalian O-Mannosylation Pathway: Glycan Structures, Enzymes, and Protein Substrates. *Biochemistry* 53: 3066–3078

Qian L, Xia Z, Zhang M, Han Q, Hu D, Qi S, Xing D, Chen Y & Zhao X (2021) Integrated Bioinformatics-Based Identification of Potential Diagnostic Biomarkers Associated with Diabetic Foot Ulcer Development. *J Diabetes Res*

2021: 1–7

Quirk J, Thornton M & Kirkpatrick P (2003) Rosuvastatin calcium. *Nat Rev Drug Discov* 2: 769–770

Ramkumar S, Raghunath A & Raghunath S (2016) Statin Therapy: Review of Safety and Potential Side Effects. *Acta Cardiol Sin* 32: 631–639

Sanvee GM, Panajatovic M V., Bouitbir J & Krähenbühl S (2019) Mechanisms of insulin resistance by simvastatin in C2C12 myotubes and in mouse skeletal muscle. *Biochem Pharmacol* 164: 23–33

Schirris TJJ, Renkema GH, Ritschel T, Voermans NC, Bilos A, van Engelen BGM, Brandt U, Koopman WJH, Beyrath JD, Rodenburg RJ, *et al* (2015) Statin-Induced Myopathy Is Associated with Mitochondrial Complex III Inhibition. *Cell Metab* 22: 399–407

Sheikh MO, Halmo SM & Wells L (2017) Recent advancements in understanding mammalian O-mannosylation. *Glycobiology* 27: 806–819

The Gene Ontology Consortium GO term elements.

Thompson PD (2003) Statin-Associated Myopathy. *JAMA* 289: 1681

Tyanova S, Temu T, Sinitcyn P, Carlson A, Hein MY, Geiger T, Mann M & Cox J (2016) The Perseus computational platform for comprehensive analysis of (prote)omics data. *Nat Methods 2016 139* 13: 731–740

Vaklavas C, Chatzizisis YS, Ziakas A, Zamboulis C & Giannoglou GD (2009) Molecular basis of statin-associated myopathy. *Atherosclerosis* 202: 18–28

Wells L (2013) The O-Mannosylation Pathway: Glycosyltransferases and Proteins

Implicated in Congenital Muscular Dystrophy. *J Biol Chem* 288: 6930–6935

Williams ZJ, Velez-Irizarry D, Gardner K & Valberg SJ (2021) Integrated proteomic and transcriptomic profiling identifies aberrant gene and protein expression in the sarcomere, mitochondrial complex I, and the extracellular matrix in Warmblood horses with myofibrillar myopathy. *BMC Genomics* 22: 438

Wu R, Long L, Zhou Q, Su J, Su W & Zhu J (2021) Identification of hub genes in rheumatoid arthritis through an integrated bioinformatics approach. *J Orthop Surg Res* 16: 458

Xiao H, Hwang JE & Wu R (2018) Mass spectrometric analysis of the N-glycoproteome in statin-treated liver cells with two lectin-independent chemical enrichment methods. *Int J Mass Spectrom* 429: 66–75